SNSPD with ultimate low system dark count rate using various cold filters

H. Shibata, K. Fukao, N. Kirigane, S. Karimoto and H. Yamamoto

***Abstract*— Suppressing the dark count rate (DCR) is one of the main issues in the development of the superconducting nanowire single-photon detector (SNSPD). Here we study the effect of suppressing DCR using the various optical bandpass filters cooled at 3 K. The DCR, which is dominated by the background blackbody radiation at room temperature through an optical fiber, can be strongly suppressed by introducing the cold filter. Using the bulk commercial filter with the bandwidth of 10 nm and the high transmission above 85 %, the DCR is improved about 29 dB with 2.4 dB decreasing of the system detection efficiency (η). The noise equivalent power (NEP) reaches 1.5×10^{-18} and the figure of merit (FOM) reaches 1.8×10^{9}. These values are compared to the results using other type of filters.**

***Index Terms*—Cold filter, Dark count rate, SNSPD, Superconducting photodetector, blackbody radiation.**

I. Introduction

SUPERCONDUCTING NANOWIRE SINGLE PHOTON DETECTOR (SNSPDs or SSPDs) have attracted much attention due to their high detection efficiency (η), low dark count rate (DCR), and low timing jitter (Δt) [1]–[4]. Now SNSPDs are being used in many fields from classical applications to quantum applications, such as free space laser communications, bio sensing, quantum key distribution (QKD), and quantum optics [5]–[10].

Although there have been many studies about improvements of the system η of SNSPD [1]–[4],[11]–[13], there are less reports about the improvements of the system DCR [14]–[17]. Since the S/N ratio of a single-photon detector is proportional to η/DCR, it is reasonable to further studies about the system DCR. We have previously shown that it is possible to suppress the system DCR down to 10^{-4} Hz (55dB suppression) using cold filters with wide blocking region [15]. Here, the system DCR reaches its theoretical limit, since the system DCR is limited by the background blackbody radiation passing through the signal passband. The demerit of using the cold optical filter is insertion loss. The system η is decreased by about 5 dB due to the insertion of the filter. Yang et al. successfully reduced the loss by fabricating the cold filter directly on the SNSPD chip [16]. In their case, the calculated loss is 0.55 dB (88 %). However, due to the imperfection of the blocking properties of the on-chip filter, the system DCR is suppressed by about 20 dB. So, at present, there is a trade-off between the high system η and the low system DCR. It is necessary to select the specifications of cold filters depending on its application. For a long distance QKD, ultralow system DCR is required since the maximum distance is limited by the S/N ratio of the detectors [7]–[9]. Actually, SNSPDs with the system DCR of 0.01 Hz using the cold filter were employed for the longest QKD experiment on fiber of 336 km [9]. On the other hand, high system η becomes essential for quantum optics applications due to the single-photon coincidence [10].

In this letter, we study the effects of suppressing system DCR using cold bulk filters with high transmission, and compare to the previous results.

II. Experiments

A. Measurement System Setup

Figure 1 shows an optical setup inside a cryocooler. A light from the outside of the cryocooler goes into it via a hermetic sealed female FC connector. The light contains the signal and

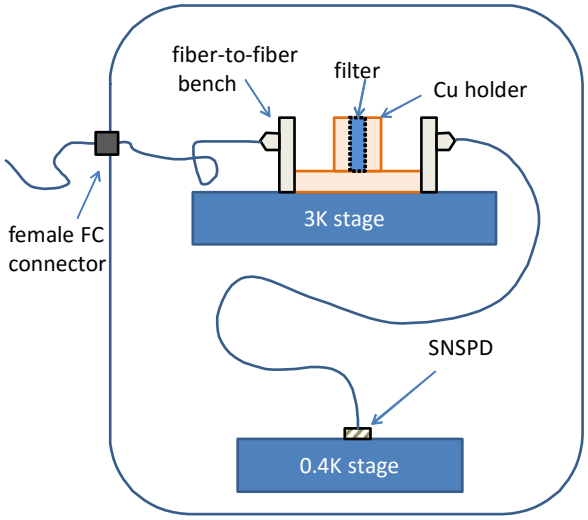

Fig. 1. Schematic of the experimental setup inside the cryocooler. The optical fiber input is connected to the fiber-to-fiber bench. The light through the fiber is converted to the light in space, transmits to the bulk filter, and is converted to the light in fiber again. The loss of the bench is below 1 dB. At the bench, the bulk filter is cooled at 3 K by a holder made of cupper.

This work was supported in part by a research granted from The Murata Science Foundation. *(Corresponding author: H. Shibata)*

H. Shibata, K. Fukao, and N. Kirigane are with the Department of Electrical and Electronic Engineering, Kitami Institute of Technology, Kitami-shi, Hokkaido, 090-8507, Japan (e-mail: shibathr@mail.kitami-it.ac.jp).

S. Karimoto and H. Yamamoto are with NTT Basic Research Laboratories, NTT Corporation, Atsugi-shi, Kanagawa 243-0198, Japan.

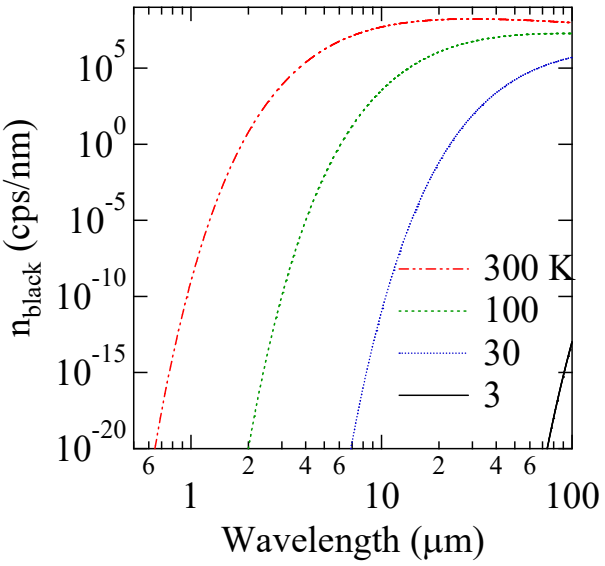

Fig. 2. Calculated photon count rate per nanometer wavelength through single-mode fiber due to the blackbody radiation.

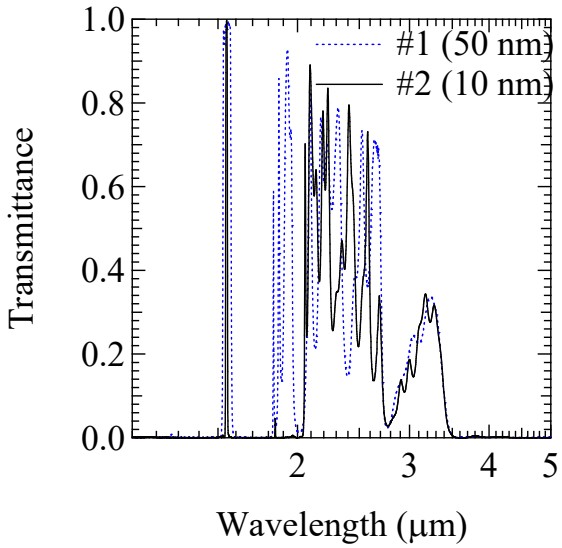

Fig. 3. Transmission spectra of the filters #1 and #2 in the wide wavelength region at room temperature.

the background blackbody radiation at room temperature. A continuous laser with the power of -98.9 dBm at 1545.6 nm is used for the light source. From the opposite side of the connector, an optical fiber is connected to the input of a fiber-to-fiber bench on a 3 K stage of the cryocooler. The light in the fiber is converted to the light in space and is transmitted to the bulk filter bench. The bulk filter is cooled at 3 K by a thermal contact with an oxygen-free copper holder. The transmitted light is converted to the light in fiber again and is collimated to the meander structure of SNSPD cooled at 0.4 K. The SNSPD is 7 nm thick NbN meander pattern on a thermally oxidized Si substrate with double side cavity structure [15]. The side of the meander is 15 × 15 μm^2 with a line and space width of 100nm. Shunt resistor is not connected. Figure 2 shows the calculated photon count rate per nanometer wavelength through single-mode fiber due to the blackbody radiation at various temperatures [14],[18]–[22]. Details of the calculation are shown in ref. [14]. From the figure, it is clear that the effect of the blackbody radiation is quite large at 300 K in the infrared region, but it becomes negligible at 3 K. In the present case, the blackbody radiation at room temperature is blocked at the filter except a passband of the filter. The loss of the bench without filter is below 1 dB at room temperature and about 1 dB at 3 K. We don't adjust the bench at low temperature.

TABLE I
SPECIFICATIONS OF THE COLD FILTERS

No.	Manufacturer, Model	Transmittance (%)	FWHM (nm)	Blocking Region (nm)
#1	Edmund 86-891	>90	50	200–1800
#2	Edmund 86-088	>85	10	400–1800
#3	Andover 200FC40	>70	20	–2400
#4	Advanced DWDM-1-40	>79	100 GHz	–

Catalog specification of the filters. #1 and #2 are bulk band-pass filters with high transmission with the center frequency at 1550 nm. #3 is the bulk band-pass filter with wide blocking region with the center frequency at 1550 nm used in [15]. #4 is the pigtailed DWDM filter with the center frequency at 1545.3 nm used in [15].

B. Cold filters

Table I summarizes catalog specifications of commercial filters used as cold filters. #1 is a bulk band-pass filter with the bandwidth of 50 nm at telecom wavelength and has a high transmittance. #2 is also a bulk band-pass filter with bandwidth of 10 nm and a high transmittance. #3 is the bulk band-pass filter with 20-nm bandwidth and has a wide blocking region used in [15]. #4 is the pigtailed dense wavelength-division multiplexer (DWDM) filter with a 100-GHz bandwidth used in [15]. Figure 3 shows the broadband transmission spectra of filter #1 and #2 at room temperature obtained using a Fourier transform infrared spectrometer. The filter #1 has a transmission window of 50 nm at 1550 nm and a transmission window between 1.8 and 3.5 μm. The filter #2 has a transmission window of 10 nm at 1550 nm and a transmission window between 2.0 and 3.5 μm. In this case, the system-DCR is dominated by the blackbody radiation at long wavelength for the filter #1 and #2, not by the blackbody radiation at signal passband. Since the filter #2 has a lower transmission at long wavelength than #1, we expect the stronger suppressing effect of system-DCR for the filter #2 than for #1. The transmission spectra of the filter #3 and #4 have been reported in [15]. The filter #3 has a wide blocking region down to 5 μm.

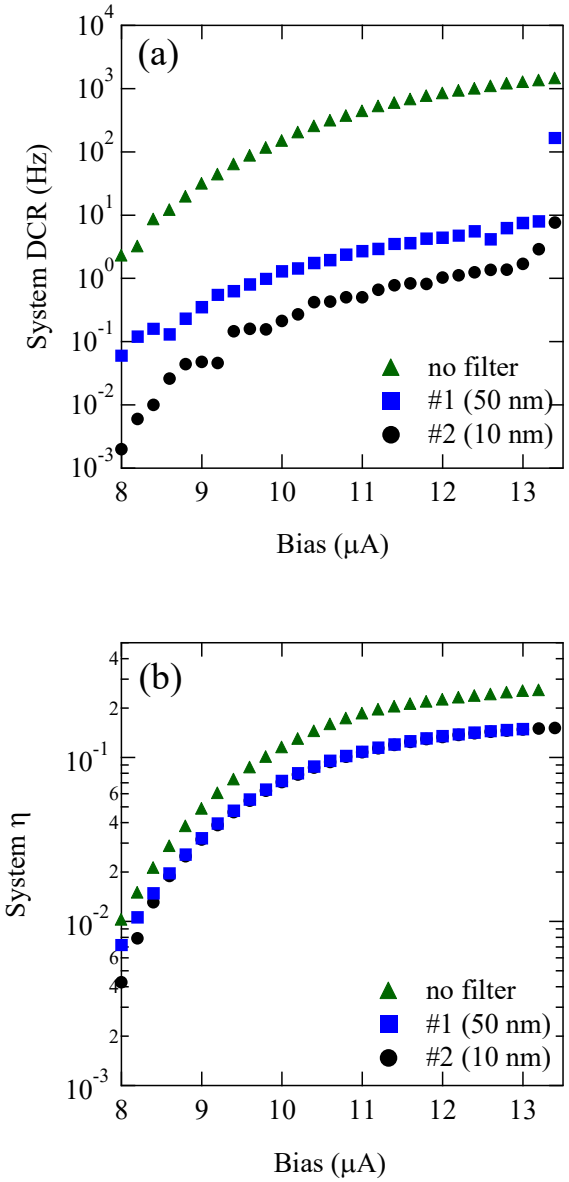

Fig. 4. (a) Bias current dependence of the system dark count rate (DCR) without filter (green triangles), with the band-pass filter #1 of 50-nm bandwidth cooled at 3 K (blue squares), with the filter #2 of 10-nm bandwidth (black circles). (b) Bias current dependence of the system detection efficiency (η) without filter (green triangles), with the band-pass filter #1 (blue squares), with the filter #2 (black circles).

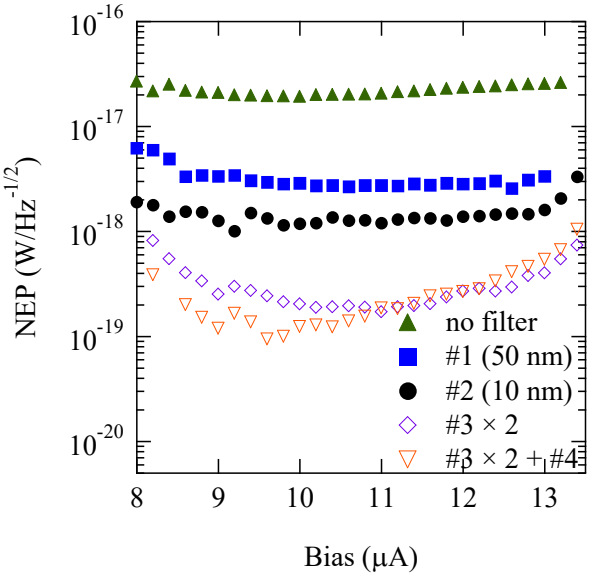

Fig. 5. Bias current dependence of the noise equivalent power (NEP) without filter (green triangles), with the filter #1 of 50-nm bandwidth (blue squares), with the filter #2 of 10-nm bandwidth (black circles), with double filters #3 of wide blocking region (purple unfilled tilted squares), and with double filters #3 and #4 of DWDM (red unfilled inverted triangles).

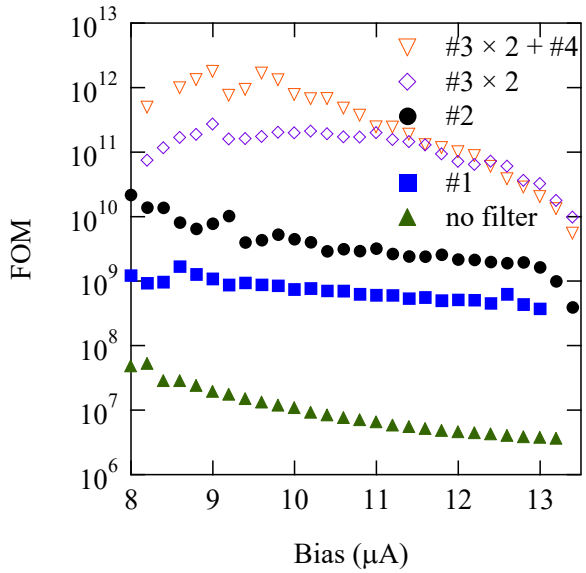

Fig. 6. Bias current dependence of the figure of merit (FOM) without filter (green triangles), with the filter #1 of 50-nm bandwidth (blue squares), with the filter #2 of 10-nm bandwidth (black circles), with the double filters #3 of wide blocking region (purple unfilled tilted squares) from [15], and with the double filters #3 and #4 of DWDM (red unfilled inverted triangles) from [15].

III. Results and Discussion

A. System DCR and η

The bias current dependence of the system DCR is shown in Fig. 4(a). The system DCR is suppressed by about 20 dB as the filter #1 is introduced (blue squares), and by about 30 dB as the filter #2 is introduced (black circles) except in the high bias region (>13 μA). The difference of the value between the filter #1 and #2 is due to the difference of the transmission at long wavelength, and not by the difference of the signal passband, as discussed before. In our previous report using pigtailed cold filters, the improvement of the system DCR is about 21 dB [14]. So, the filter #2 is more effective than the pigtailed filters and the on-chip filter for improving system DCR. On the other hand, the value is less effective compared to the results using filters with wide blocking region (#3 and #4), and confirms the effect of blackbody radiation at long wavelength.

Figure 4(b) summarizes the bias current dependence of the system η of the filter #1 and #2. By incorporating the filter #1

and #2, system η decreases by about 2.2 and 2.4 dB, respectively. These values are higher than the on-chip filter (0.55 dB), but are lower than the other bulk or pigtailed cold filters. The loss of the filters is about 2.7 dB in pigtailed filters, about 3–4 dB in double filters #3, and about 5 dB in double filters #3 and the filter #4.

B. NEP and FOM

One of the well-known parameter to characterize the performance of an ultrasensitive detector is the noise equivalent power (NEP). In the case of single-photon detectors, NEP is expressed as $NEP = h\nu\,(2 \cdot DCR)^{1/2}/\eta$, where $h\nu$ is the photon energy. Figure 5 shows the bias current dependences of NEP of various cold filters. The NEP decreases about 9 dB for the filter #1 and 12 dB for #2, and has a little bias dependence. For the filter #3 and #4, the NEP decreases lower than the filter #1 and #2, and the NEP reaches 1.7×10^{-19} for double filters #3 at 11 μA, and 9.6×10^{-20} for double filters #3 and the filter #4 at 9.6 μA, respectively. These values are the lowest NEP values for SNSPD.

A figure of merit (FOM) is another parameter to characterize the performance of single-photon detectors. It is defined as $FOM = \eta/(DCR\Delta t)$. FOM is well suited for the threshold single-photon detectors, since it is dimensionless, represents the S/N ratio of the detectors, and is related to a minimal timing interval [3],[4],[14],[15]. We assume that the changes of Δt due to introducing the filter are negligible and use the same data as [15]. Figure 6 summarizes the bias current dependences of FOM for the filter #1 and #2. Here, we also plot the FOM for the filter #3 and #4 for comparison. From the figure, it is revealed that the FOM is improved by about 20 dB for the filter #1 and about 27 dB for #2, respectively. These values are lower than that of the filter #3 and #4 as expected.

In conclusion, we investigate the effect of system DCR with various cold filters. Among them, the filter #2 can be used as a new cold filter for the suppression of the system DCR with moderate insertion loss. By simply introducing the cold filter, we can easily improve the S/N ratio of the SNSPD about 27 dB. The method can be applied to many applications, where ultrasensitive single-photon detections are required. The experimental setup of the bulk cold filter is explained in detail.

ACKNOWLEDGMENT

The authors would like to thank T. Tamamura and T. Ashida for their technical support.

REFERENCES

[1] G. N. Gol'tsman, O. Okunev, G. Chulkova, A. Lipatov, A. Semenov, K. Smirnov, B. Voronov, A. Dzardanov, C. Williams, and R. Sobolewski, "Picosecond superconducting single-photon optical detector," Appl. Phys. Lett. vol. 79, pp. 705-707, 2001.

[2] C. M. Natarajan, M. G. Tanner, and R. H. Hadfield, "Superconducting nanowire single-photon detectors: physics and applications," Supercond. Sci. Technol. vol. 25, 063001, 2012.

[3] R. H. Hadfield, "Single-photon detectors for optical quantum information applications," Nat. Photon. vol. 3, pp. 696-705, 2009.

[4] M. D. Eisaman, J. Fan, A. Migdall, and S. V. Polyakov, "Invited Review Article: Single-photon sources and detectors," Rev. Sci. Instrum. vol. 82, 071101, 2011.

[5] N. R. Gemmell, A. McCarthy, B. Liu, M. G. Tanner, S. D. Dorenbos, V. Zwiller, M. S. Patterson, G. S. Buller, B. C. Wilson, and R. H. Hadfield, "Singlet oxygen luminescence detection with a fiber-coupled superconducting nanowire single-photon detector," Opt. Express vol. 21, pp. 5005–5013, 2013.

[6] A. Biswas, J. M. Kovalik, M. Srinivasan, M. Shaw, S. Piazzolla, M. W. Wright, and W. H. Farr, "Deep space laser communications," Proc. of SPIE vol. 9739, 97390Q-1, 2016.

[7] H. Takesue, S. W. Nam, Q. Zhang, R. H. Hadfield, T. Honjo, K. Tamaki, and Y. Yamamoto, "Quantum key distribution over a 40-dB channel loss using superconducting single-photon detectors," Nat. Photon. vol. 1, pp. 343-348, 2007.

[8] S. Wang, W. Chen, J. F. Guo, Z. Q. Yin, H. W. Li, Z. Zhou, G. C. Guo, and Z. F. Han, "2 GHz clock quantum key distribution over 260 km of standard telecom fiber," Opt. Lett. vol. 37, pp. 1008-1010, 2012.

[9] H. Shibata, T. Honjo, and K. Shimizu, "Quantum Key Distribution over a 72 dB channel loss using ultralow dark count superconducting single-photon detectors," Opt. Lett. vol. 39, pp. 5078-5081, 2014.

[10] T. Guerreiro, F. Monteiro, A. Martin, J. B. Brask, T. Vértesi, B. Korzh, M. Caloz, F. Bussières, V. B. Verma, A. E. Lita, R. P. Mirin, S. W. Nam, F. Marsilli, M. D. Shaw, N. Gisin, N. Brunner, H. Zbinden, and R. T. Thew, "Demonstration of Einstein-Podolsky-Rosen Steering Using Single-Photon Path Entanglement and Displacement-Based Detection," Phys. Rev. Lett. vol. 117, 070404 ,2016.

[11] D. Rosenberg, A. J. Kerman, R. J. Molnar, and E. A. Dauler, "High-speed and high-efficiency superconducting nanowire single photon detector array," Opt. Express vol. 21, pp. 1440-1447, 2013.

[12] F. Marsili, V. B. Verma, J. A. Stern, S. Harrington, A. E. Lita, T. Gerrits, I. Vayshenker, B. Baek, M. D. Shaw, R. P. Mirin, and S. W. Nam, "Detecting single infrared photons with 93 % system efficiency," Nat. Photon. vol. 7, pp. 210-214, 2013.

[13] S. Miki, T. Yamashita, H. Terai, and Z. Wang, "High performance fiber-coupled NbTiN superconducting nanowire single photon detectors with Gifford-McMahon cryocooler", Opt. Express vol. 21, pp. 10208-10214, 2013.

[14] H. Shibata, K. Shimizu, H. Takesue, and Y. Tokura, "Superconducting nanowire single-photon detector with ultralow dark count rate using cold optical filters," Appl. Phys. Express vol. 6, 072801, 2013.

[15] H. Shibata, K. Shimizu, H. Takesue, and Y. Tokura, "Ultimate low system dark-count rate for superconducting nanowire single-photon detector," Opt. Lett. vol. 40, pp. 3428-3431, 2015.

[16] X. Yang, H. Li, W. Zhang, L. You, L. Zhang, X. Liu, Z. Wang, W. Peng, X. Xie, and M. Jiang, "Superconducting nanowire single photon detector with on-chip bandpass filter," Opt. Express vol. 22, pp. 16267-16272, 2014.

[17] S. Chen, L. You, W. Zhang, X. Yang, H. Li, L. Zhang, Z. Wang, and X. Xie, "Dark counts of superconducting nanowire single-photon detector under illumination," Opt. Express vol. 23, pp. 10786-10793, 2015.

[18] K. Smirnov, Y. Vachtomin, A. Divochiy, A. Antipov, and G. Goltsman, "Dependence of dark count rates in superconducting single photon detectors on the filtering effect of standard single mode optical fibers," Appl. Phys. Express vol. 8, 022501, 2015.

[19] T. Yamashita, S. Miki, W. Qiu, M. Fujiwara, M. Sasaki, and Z. Wang, "Temperature dependent performances of superconducting nanowire single-photon detectors in an ultralow-temperature region," Appl. Phys. Express vol. 3, 102502, 2010.

[20] D. Fukuda, G. Fujii, T. Numata, K. Amemiya, A. Yoshizawa, H. Tsuchida, H. Fujino, H. Ishii, T. Itatani, S. Inoue, and T. Zama, "Titanium Superconducting Photon-Number-Resolving Detector," IEEE Trans. Appl. Supercond. vol. 21, pp. 241-245, 2011.

[21] A. J. Miller, A. Lita, D. Rosenberg, S. Gruber, and S. W. Nam, "SUPERCONDUCTING PHOTON NUMBER RESOLVING DETECTORS: PERFORMANCE AND PROMISE," Proc. 8th Int. Conf. Quantum Communication, Measurement and Computing (QCMC'06), pp. 445-450, Tsukuba, Japan, Nov. 2006.

[22] A. Engel, A. Semenov, H. W. Hübers, K. Ilin, and M. Siegel, "Dark counts of a superconducting single-photon detector," Nucl. Instrum. Meth. Phys. Res. Sect. A 520, pp. 32–35, 2004.